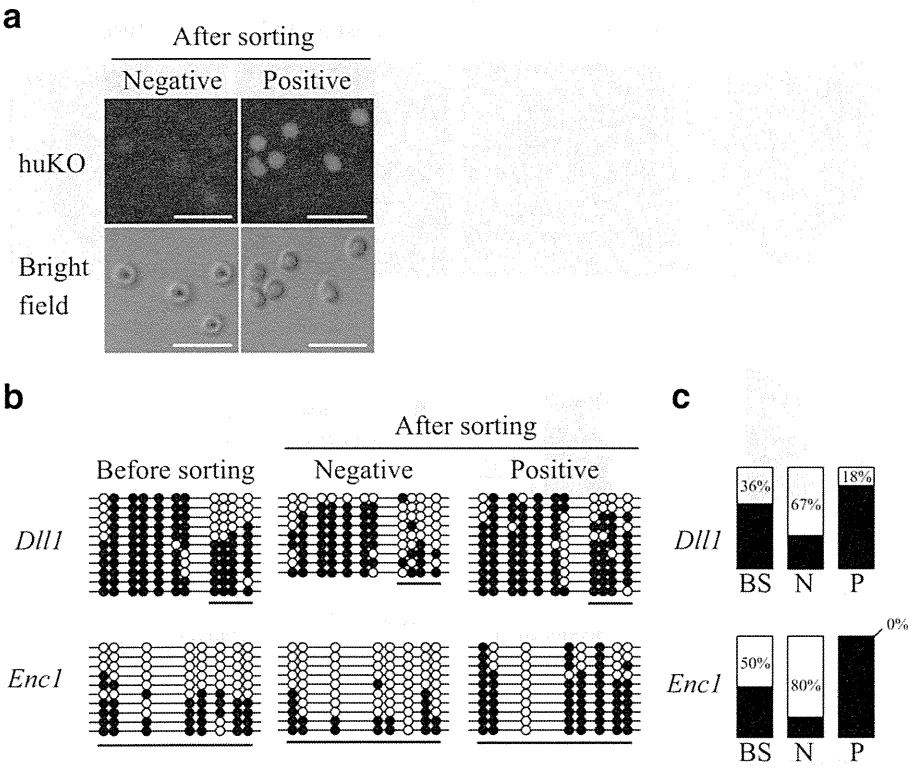

FIG. 4. DNA methylation status of huKO-negative cells after sorting of Porco Rosso-4. (**a**) The huKO-negative and huKO-positive cells of Porco Rosso-4 iPSC line after sorting. Scale bar = 50 μm. (**b**) DNA methylation status of *Dll1* and *Enc1* before and after sorting (huKO-negative and huKO-positive). Open and closed circles indicate unmethylated and methylated CpG dinucleotides, respectively. (**c**) The percentage of (hypomethylated clones)/(all sequenced clones) in the underlined regions of Figure 4b. Hypomethylated clones were defined on the basis of the number of unmethylated CpGs underlined below the circles in each sequenced clone. At the *Dll1* locus, the DNA methylation statuses of four CpGs were clearly different between the bulk Porco Rosso-4 line and PFF in Figure 2, whereas the other CpGs were almost fully methylated in all of the sequenced clones, indicating that the methylation statuses of the four selected CpGs in the underlined region were informative enough for evaluating the ratio of properly reprogrammed cells in huKO-negative and huKO-positive fractions. Thus, sequenced clones with three or more unmethylated CpGs in the four CpGs were designated as hypomethylated at the *Dll1* locus. At the *Enc1* locus, about half of the sequenced clones exhibited six or more unmethylated CpGs within the eight CpGs examined in the bulk Porco Rosso-4 line (Fig. 2). However, the other sequenced clones were almost fully methylated at the eight CpGs. Thus, sequenced clones exhibiting six or more unmethylated CpGs were designated as hypomethylated to strictly evaluate properly reprogrammed cells at the *Enc1* locus. With respect to the other four EShypo-T-DMRs (*Ctnnb1*, *Sall4*, *Tle4*, and *Nebl*) analyzed in Figure 2, the DNA methylation statuses of hypomethylated CpGs in bulk Porco Rosso-4 cells did not differ between huKO-negative and huKO-positive cells (Supporting Information Fig. 2). Black and white bars indicate the ratio of hypermethylated and hypomethylated clones, respectively. BS, before sorting; N, huKO-negative cells; P, huKO-positive cells.

remained unchanged compared with FBS-cultured controls.

Improvement of the DNA methylation status of Porco Clawn cells by culture under SF+2i conditions was confirmed by sodium bisulfite sequencing (Fig. 5b). *Sall4*, *Hexb*, and *Zfp64*, all of which are Oct3/4-targets, were hypermethylated in the presence of FBS, whereas demethylation occurred under the SF+2i conditions. By contrast, demethylation at *Hexb* and *Zfp64* was much less pronounced in the 5-aza-dC-treated cells (Fig. 5b). These results suggest that the SF+2i condition was the most effective of those tested for reprogramming of the 36-gene set. Demethylation also occurred in the SF+2i-treated cells at the *Dll1* and *Enc1* loci (Supporting Information Fig. 3a), whereas a portion of cells remained hypermethylated at the *Dll1* locus (Supporting Information Fig. 3b). In addition, DNA methylation analysis revealed that a proportion of cells still needed to be reprogrammed at the *Enc1* locus even after SF+2i treatment.

To examine whether SF+2i culture conditions are effective in improving pluripotency scores, we cultured Porco Clawn, in addition to several other iPSC lines, under the same conditions (FBS, SF, and SF+2i), and DNA methylation status was analyzed by COBRA assay (Fig. 5c). Of note, the pluripotency scores of all the three gene groups (Oct3/4-targets, KSM-targets, and non-targets) were increased in Porco Rosso-4 cells under SF+2i condition compared with FBS, or SF

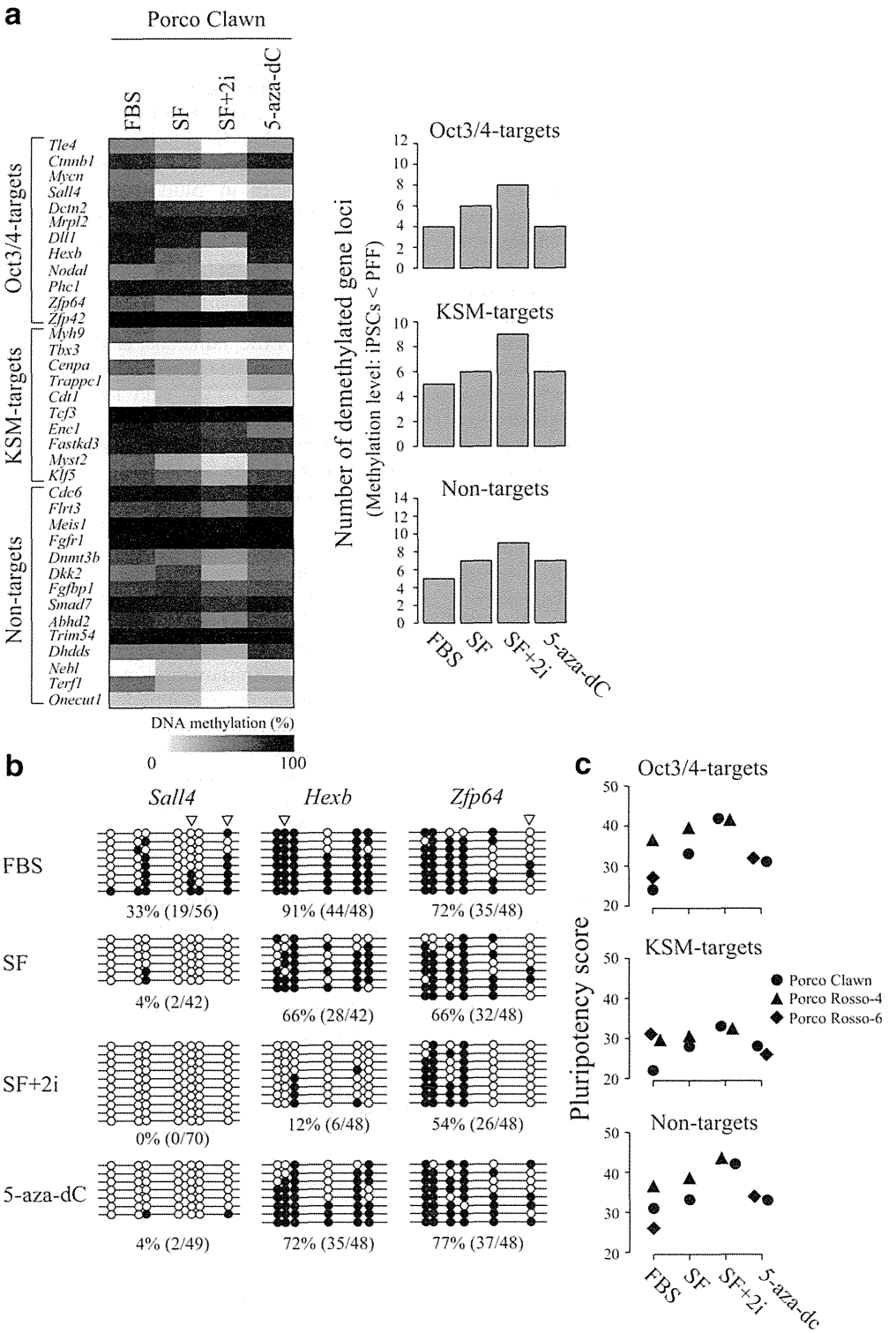

FIG. 5. Continued

conditions. Thus, SF+2i treatment is effective for multiple porcine iPSC lines.

DISCUSSION

The porcine iPSCs analyzed in this study exhibited LIF-dependent self-renewal and a round morphology, similar to mouse ESCs (Fujishiro *et al.*, 2013). The expression patterns of several pluripotency-related marker genes, including *Oct3/4*, were also similar among the iPSC lines. As it is intended that these iPSC lines will be used for applications such as chimera formation (Okita *et al.*, 2007) and transplantation experiments (Kobayashi *et al.*, 2010; Usui *et al.*, 2012), it is important that they are able to contribute to the ICM of the blastocyst embryos. In this context, a simple index, other than morphology and marker gene expression, correlating with ICM contribution efficiency is required to allow pre-screening to determine which iPSC lines are appropriate for use in labor- and cost-intensive transplantation experiments. We previously reported that mouse iPSC lines with high chimera-forming ability (Aoi *et al.*, 2008) have DNA methylation profiles close to those of ESCs (Sato *et al.*, 2010). In this study, we focused on the DNA methylation profile of mouse EShypo-T-DMRs and determined a 36-gene set applicable to porcine iPSC lines. The pluripotency scores, based on the DNA methylation profile of the 36-gene set, were revealed to differ among iPSC lines that were indistinguishable by morphology or marker gene expression. Moreover, the iPSC line with the highest pluripotency score contributed to the ICM as assessed by a chimera formation experiment, whereas the iPSC line with the lowest score contributed much less efficiently to the ICM. Collectively, the DNA methylation profile of the 36-gene set derived from mouse EShypo-T-DMRs correlated with the ability to contribute to the ICM of blastocyst embryos.

In the course of mouse iPSC establishment, reprogramming for activation is important for genes such as endogenous *Oct3/4* and target genes of Yamanaka factors (Oct3/4, Sox2, Klf4, and c-Myc) (Okita *et al.*, 2007; Takahashi and Yamanaka, 2006). In this study, we categorized the 36-gene set into three groups (Oct3/4-targets, KSM-targets, and non-targets), and analyzed DNA methylation status in porcine iPSCs. Among the three groups, differences in pluripotency score were most apparent in the Oct3/4-target genes. The Oct3/4-target group contains genes that are important for the maintenance of pluripotency in stem cells. For example, *Sall4* is an Oct3/4-target gene (Chen *et al.*, 2008; Sakaki-Yumoto *et al.*, 2006; Tsubooka *et al.*, 2009) and was hypomethylated in the porcine iPSC line exhibiting both a high pluripotency score and efficient contribution to ICM. Differences in pluripotency scores among the examined iPSC lines were less significant in the KSM-target group than the Oct3/4-target group. Non-target genes can be thought of as downstream targets of the four Yamanaka factors, thereby non-target genes should be secondarily reprogrammed after activation of the primary targets of the Yamanaka factors. Thus, the pluripotency score of non-target genes was relatively high in iPSCs with high Oct3/4- and KSM-target scores, most likely indicating the activation of the primary target genes. Therefore, although pluripotency scores of Oct3/4-target genes can be considered as the most important index for evaluation of porcine iPSCs, the DNA methylation profiles of all three groups making up the 36 genes are required for evaluation with high accuracy.

For establishing mouse iPSCs, 2i treatment has been reported as effective for obtaining high-quality lines (Buehr *et al.*, 2008; Hanna *et al.*, 2009; Li *et al.*, 2008). The 2i consists of MEK- and GSK3b-inhibitors, both of which prevent differentiation of mouse ESCs. In the porcine iPSC lines we examined, 2i-treatment effectively induced demethylation of the 36-gene set, with a consequent increase in pluripotency scores. Since an increased pluripotency score indicates cells with closer characteristics to those of pluripotent stem cells, such as mouse ESCs, the DNA methylation profile of the 36-gene set is useful for detection of improvements of porcine iPSC lines. In contrast, treatment of 5-aza-dC was less effective for improvement of pluripotency scores, implying that simple DNA demethylation by such compounds is insufficient. Taken together, DNA methylation profiling is useful for evaluation of characteristic changes of porcine iPSCs.

Reprogramming of endogenous pluripotency-related genes such as *Oct3/4* is crucial for stably maintaining iPSCs. By contrast, the first report of mouse iPSCs (Fbx15 iPSCs) observed incomplete demethylation of the endogenous *Oct3/4* region and the cells were not transmitted through the germline (Takahashi and Yamanaka, 2006), whereas superior germline-transmittable iPSC lines (Nanog iPSCs) showed complete demethylation of

FIG. 5. Improvement of DNA methylation status under different culture conditions. (**a**) DNA methylation status of Porco Clawn cells cultured in the presence of FBS, or in serum-free (SF), SF + 2i, or 5-aza-dC conditions was analyzed by COBRA assay; the methylation level is represented as a heatmap (left panel). The number of demethylated genes in each culture condition is shown in the right panel. (**b**) DNA methylation status of three Oct3/4-target genes (*Sall4*, *Hexb*, and *Zfp64*) in Porco Clawn cells cultured under different conditions analyzed by sodium bisulfite sequencing. Open and closed circles indicate unmethylated and methylated CpG dinucleotides, respectively. Arrowheads indicate CpG sites analyzed by COBRA assay. The methylation level (%) was calculated as methylated CpGs/all examined CpGs. (**c**) DNA methylation status in Porco Rosso-4 cells cultured under SF or SF + 2i conditions and in Porco Rosso-6 cultured in the presence of 5-aza-dC was analyzed by COBRA assay. Pluripotency scores of the iPSC lines cultured under each condition were plotted for the three gene-groups (Oct3/4-targets, KSM-targets, and non-targets).

the endogenous pluripotency-related genes including *Oct3/4* (Okita *et al.*, 2007). We previously reported that the endogenous *Oct3/4* promoter region was relatively hypermethylated in the same porcine iPSC lines that were examined in this study (Fujishiro *et al.*, 2013). However, one iPSC line that we analyzed contained cells showing reprogrammed and hypomethylated status within the whole examined endogenous *Oct3/4* locus, suggesting that a small population of the cells were activated at the endogenous *Oct3/4* locus. In mouse ESCs, a 1.5-fold increase or two-fold decrease in endogenous *Oct3/4* expression led to cellular differentiation (Niwa *et al.*, 2000). Therefore, the appropriate expression level of endogenous *Oct3/4* is important for maintenance of pluripotency. In the pig, however, no *bona fide* pluripotent stem cells, such as mouse ESCs, have been described to date; thus, the appropriate expression level of endogenous *Oct3/4* remains to be determined. Based on the bisulfite sequencing data of endogenous *Oct3/4* in our previous study (Fujishiro *et al.*, 2013) and several Oct3/4-targets in this study, a proportion of the cells appear to be properly reprogrammed in the iPSC lines we examined. In addition, the finding that huKO-negative cells, which are likely closer to pluripotent cells (Fujishiro *et al.*, 2013), exhibited hypomethylation of EShypo-T-DMRs compared with the bulk iPSC line further support the usefulness of DNA methylation profile. Thus, DNA methylation analysis can evaluate the ratio of properly reprogrammed cells in each iPSC line without reference cells such as ESCs in the case of mouse iPSCs.

The porcine iPSC lines examined in this study were likely heterozygous and contained both properly and improperly reprogrammed cells, even after SF/2i-treatment, as shown by the measurement of the DNA methylation patterns of several EShypo-T-DMRs. For aggregation experiments, one iPSC colony large enough to be picked up was dissociated into single cells and aggregated with early embryonic cells. Under the present culture conditions, properly reprogrammed cells such as huKO-negative cells, which we proved to have better characteristics as stem cells (Fujishiro *et al.*, 2013), exhibited slower proliferation than improperly reprogrammed cells (data not shown). This implies that visible iPSC colonies, which can be used for aggregation experiments to analyze ICM contribution, contain substantial numbers of improperly reprogrammed cells due to higher proliferation potential than properly reprogrammed cells. Thus, the data demonstrating the ICM contribution of iPSCs in this study may have underestimated the ratio of properly reprogrammed cells that could be deduced from DNA methylation analysis. In this study, we identified several genes whose methylation profiles could be used to evaluate the ratio of properly reprogrammed cells. Thus, we will be able to identify appropriate culture conditions for the maintenance of properly reprogrammed cells by using the DNA methylation profiles of these genes.

In this study, we focused on the DNA methylation profile of the 36-gene set derived from EShypo-T-DMRs and established a new index for evaluation of porcine iPSCs correlating with their efficient contribution to the ICM of blastocysts. We provide proof-of-principle of the concept that mouse EShypo-T-DMR information is applicable to evaluate porcine iPSC lines. The gene set we used in this study is effective on validation of stemness under in vitro culture condition and in blastocyst stage embryos as one aspect of pluripotency. However, the other aspect of pluripotency to have broad lineage potential is also important but cannot be assessed by the gene set used in this study. We previously identified differentiated-tissue-specific hypomethylated loci (Tissuehypo-T-DMRs), which are related to certain specific somatic cell lineages and are hypermethylated in mouse ESCs (Sato *et al.*, 2010). By selecting another porcine gene set from Tissuehypo-T-DMRs in addition to the 36-gene set examined in this study, we will be able to perform more strict evaluation of porcine iPSCs in terms of pluripotency of both stemness and broad lineage potential. Since our previous findings indicated that hundreds of mouse EShypo- and Tissuehypo-T-DMRs could be used for evaluation of mouse iPSCs, we anticipate deriving further information about EShypo- and Tissuehypo-T-DMRs in multiple porcine iPSC lines with higher accuracy using next generation sequencer to perform ultra-deep bisulfite sequencing.

In conclusion, information regarding DNA methylation derived from mouse EShypo-T-DMRs is a feasible index for evaluation of porcine iPSCs as a pre-screening tool, distinct from morphology and marker gene expression analysis. Evaluation of porcine iPSC lines by DNA methylation analysis is simple and time/cost-saving. The concept of evaluation of iPSCs by DNA methylation profile is readily applicable to other mammalian cells, including human iPSCs/ESCs, which cannot be evaluated by chimera formation for ethical reasons.

METHODS

Animal Care

All of the animal experiments in this study were approved by the Institutional Animal Care and Use Committee of Meiji University (IACUC-11-1).

Chemicals

Chemicals were purchased from the Sigma Chemical Co. (St. Louis, MO), unless otherwise indicated.

Porcine iPSCs

Establishment of porcine iPSCs was described previously (Fujishiro *et al.*, 2013). Porcine iPSC lines, Porco

Rosso-4, −6, −622-14, and Epistem-like B9-2-5, expressing humanized Kusabira-Orange (huKO) were derived from PFF of huKO-transgenic pigs (Matsunari *et al.*, 2008). Porco Clawn iPSC line was derived from PFF of Clawn miniature pigs (Japan Farm, Kagoshima, Japan). All the iPSC lines were maintained in knockout DMEM medium (Invitrogen, Rockville, MD) containing 15% fetal bovine serum (FBS, Invitrogen) or knockout serum replacement (KSR, Invitrogen), 1% NEAA (Invitrogen), 1% glutamax-L (Invitrogen), 100 μM 2-mercaptoethanol (Invitrogen), 50 U/ml penicillin, 50 μg/ml streptomycin, 10 μM forskolin (Biomol, Farmingdale, NY), and 0.5% porcine LIF with or without 5 μM 5-aza-2′-deoxycytidine (5-aza-dC) for 10 days and two signal-transduction inhibitors (2i) of 0.5 μM PD0325901 and 3 μM CHIR99021 for three weeks on MMC-treated STO cells. huKO-negative and huKO-positive cells of Porco Rosso-4 were sorted by BD FACS Aria (Becton Dickinson, NJ).

COBRA Assay and Sodium Bisulfite Genomic Sequencing

DNA methylation analysis by COBRA assay was performed based on our previous results (Sato *et al.*, 2010) focusing on 58 genes that were hypomethylated in mouse ESCs. Genomic DNA was purified using the DNeasy Blood & Tissue Kit (Qiagen, Hilden, Germany), and digested with a restriction enzyme *Hind* III (Takara Bio, Shiga, Japan). Digested genomic DNA was purified with a QIAquick Gel Extraction Kit (Qiagen), and bisulfite reactions were performed using the EZ DNA Methylation-Direct Kit (Zymo Research, Irvine, CA). Bisulfite-treated DNA was amplified with BioTaq HS DNA polymerase (Bioline, London, UK) using specific gene primers (Supporting Information Table 1). Primer sequences are based on the porcine genome assembly, Sscrofa9.2 (November 2009 build) from the UCSC genome database. PCR was performed under the following conditions: 95°C, 10 min; 40 cycles of 95°C, 30 s; 60°C, 30 s; 72°C, 1 min; final extension 72°C, 2 min. Amplified PCR products were digested with *Hpy* CH4 IV (New England BioLabs, Beverly, MA) at 37°C for 3 h, or *Taq* I (Takara Bio) at 65°C for 3 h and analyzed by electrophoresis. DNA methylation levels were calculated using the formula: estimated methylation degree (%) = $100 \times I^{C}/(I^{C} + I^{UC})$, where I^{C} and I^{UC} represent intensities of digested and undigested bands, respectively. The intensities of bands were determined using ImageJ software provided by the National Institutes of Health (http://rsb.info.nih.gov/ij/). COBRA assay was independently performed twice for all samples. PCR products were cloned into the pGEM T-Easy vector (Promega, Madison, WI), and 10 to 16 clones sequenced to determine DNA methylation status.

Preparation of Porcine Parthenogenetic Embryos

Porcine parthenogenetic embryos were generated as reported previously (Matsunari *et al.*, 2008). Briefly, porcine ovaries were collected at local abattoirs. In vitro maturated oocytes with expanded cumulus cells were treated with 1 mg/ml of hyaluronidase dissolved in Tyrode's lactose medium containing 10 mM HEPES and 0.3% (w/v) polyvinylpyrrolidone (HEPES-TL-PVP), and separated from the cumulus cells by gentle pipetting. Oocytes with evenly granulated ooplasm and an extruded first polar body were selected for subsequent experiments. Oocytes were transferred to an activation solution consisting of 0.3 M mannitol (Nacalai Tesque, Kyoto, Japan), 50 μM $CaCl_2$, 100 μM $MgCl_2$, and 0.01% (w/v) PVA, and activated by applying a single direct current pulse (150 V/mm, 100 μsec) using an electrical pulsing machine (LF201; Nepa Gene, Chiba, Japan). Activated oocytes were cultured and treated with 5 μg/ml cytochalasin B for 3 h to suppress extrusion of the second polar body followed by in vitro culture for up to 4 days to obtain parthenogenetic host embryos at 4 to 8-cell- and morula-stages. In vitro culture of parthenogenetic embryos was performed in porcine zygote medium-5 (PZM-5; Research Institute for the Functional Peptides, Yamagata, Japan) under paraffin oil (Kanto Chemical, Tokyo, Japan) in a humidified atmosphere of 5% CO_2, 5% O_2, and 90% N_2 at 38.5°C.

Production of Aggregated Embryos

Parthenogenetic embryos at 4- to 8-cell (day 3) or morula (day 4) stages were used as host embryos for aggregation of iPSCs. Host 4- to 8-cell embryos or morulae were decompacted by incubation in Ca^{2+}/Mg^{2+}-free Dulbecco phosphate-buffered saline (DPBS; Nissui, Tokyo, Japan) containing 0.1 mM EDTA-2Na and 0.01% (w/v) PVA for 15–20 min, followed by removal of the zona pellucidae by digestion with 0.25% (w/v) pronase in DPBS. Small clumps (~30 cells) of iPSCs were isolated from the feeder layer and kept in a drop of 21 mM Hepes-buffered MEM (Invitrogen) supplemented with 5 mg/ml BSA (Sigma) (MEM-HEPES). Aggregation of iPSC clumps and host embryos was carried out using the micro-well method (Nagy and Rossant, 1993). Each clump of iPSCs was aggregated with host blastomeres isolated from two parthenogenetic embryos at 4- to 8-cell or morula stages.

Some of the parthenogenetic host embryos were aggregated with ICM clumps isolated from parthenogenetic blastocysts on day 6 by immunosurgery as described previously (Nagashima *et al.*, 2004). Isolated ICM cells were labeled with fluorescent carbocyanine dye (DiI, Takara Bio) for 30 min, followed by thorough washing with MEM-HEPES.

Embryos produced by the aggregation method were cultured for 48–72 h in PZM-5. Blastocysts at day 6

were observed by confocal microscopy to analyze the incorporation of the donor cells into the ICM. Images of blastocysts placed in a drop of DPBS containing 5 μg/ml Hoechst 33342 were taken using a confocal fluorescence microscope (FV-1000; Olympus, Tokyo, Japan).

ACKNOWLEDGMENTS

The authors acknowledge Dr. Masaki Nagaya for helpful discussions on this manuscript and Mr. Taisuke Matsuda for technical help.

LITERATURE CITED

Aoi T, Yae K, Nakagawa M, Ichisaka T, Okita K, Takahashi K, Chiba T, Yamanaka S. 2008. Generation of pluripotent stem cells from adult mouse liver and stomach cells. Science 321:699-702.

Brons IG, Smithers LE, Trotter MW, Rugg-Gunn P, Sun B, Chuva de Sousa Lopes SM, Howlett SK, Clarkson A, Ahrlund-Richter L, Pedersen RA, Vallier L. 2007. Derivation of pluripotent epiblast stem cells from mammalian embryos. Nature 448:191-195.

Buehr M, Meek S, Blair K, Yang J, Ure J, Silva J, McLay R, Hall J, Ying QL, Smith A. 2008. Capture of authentic embryonic stem cells from rat blastocysts. Cell 135: 1287-1298.

Chen X, Xu H, Yuan P, Fang F, Huss M, Vega VB, Wong E, Orlov YL, Zhang W, Jiang J, Loh YH, Yeo HC, Yeo ZX, Narang V, Govindarajan KR, Leong B, Shahab A, Ruan Y, Bourque G, Sung WK, Clarke ND, Wei CL, Ng HH. 2008. Integration of external signaling pathways with the core transcriptional network in embryonic stem cells. Cell 133:1106-1117.

Ebert AD, Yu J, Rose FF Jr, Mattis VB, Lorson CL, Thomson JA, Svendsen CN. 2009. Induced pluripotent stem cells from a spinal muscular atrophy patient. Nature 457:277-280.

Ezashi T, Telugu BP, Alexenko AP, Sachdev S, Sinha S, Roberts RM. 2009. Derivation of induced pluripotent stem cells from pig somatic cells. Proc Natl Acad Sci USA 106:10993-10998.

Fujishiro SH, Nakano K, Mizukami Y, Azami T, Arai Y, Matsunari H, Ishino R, Nishimura T, Watanabe M, Abe T, Furukawa Y, Umeyama K, Yamanaka S, Ema M, Nagashima H, Hanazono Y. 2013. Generation of naive-like porcine-induced pluripotent stem cells capable of contributing to embryonic and fetal development. Stem Cells Dev 22:473-482.

Golob JL, Paige SL, Muskheli V, Pabon L, Murry CE. 2008. Chromatin remodeling during mouse and human embryonic stem cell differentiation. Dev Dyn 237:1389-1398.

Hanna J, Markoulaki S, Mitalipova M, Cheng AW, Cassady JP, Staerk J, Carey BW, Lengner CJ, Foreman R, Love J, Gao Q, Kim J, Jaenisch R. 2009. Metastable pluripotent states in NOD-mouse-derived ESCs. Cell Stem Cell 4:513-524.

Hattori N, Nishino K, Ko YG, Hattori N, Ohgane J, Tanaka S, Shiota K. 2004. Epigenetic control of mouse Oct-4 gene expression in embryonic stem cells and trophoblast stem cells. J Biol Chem 279: 17063-17069.

Hayashi K, Ohta H, Kurimoto K, Aramaki S, Saitou M. 2011. Reconstitution of the mouse germ cell specification pathway in culture by pluripotent stem cells. Cell 146:519-532.

Hayashi K, Ogushi S, Kurimoto K, Shimamoto S, Ohta H, Saitou M. 2012. Offspring from oocytes derived from in vitro primordial germ cell-like cells in mice. Science 338:971-975.

Ikegami K, Ohgane J, Tanaka S, Yagi S, Shiota K. 2009. Interplay between DNA methylation, histone modification and chromatin remodeling in stem cells and during development. Int J Dev Biol 53:203-214.

Imaizumi Y, Okada Y, Akamatsu W, Koike M, Kuzumaki N, Hayakawa H, Nihira T, Kobayashi T, Ohyama M, Sato S, Takanashi M, Funayama M, Hirayama A, Soga T, Hishiki T, Suematsu M, Yagi T, Ito D, Kosakai A, Hayashi K, Shouji M, Nakanishi A, Suzuki N, Mizuno Y, Mizushima N, Amagai M, Uchiyama Y, Mochizuki H, Hattori N, Okano H. 2012. Mitochondrial dysfunction associated with increased oxidative stress and alpha-synuclein accumulation in PARK2 iPSC-derived neurons and postmortem brain tissue. Mol Brain 5:35.

Imamura M, Miura K, Iwabuchi K, Ichisaka T, Nakagawa M, Lee J, Kanatsu-Shinohara M, Shinohara T, Yamanaka S. 2006. Transcriptional repression and DNA hypermethylation of a small set of ES cell marker genes in male germline stem cells. BMC Dev Biol 6:34.

Inoue H, Yamanaka S. 2011. The use of induced pluripotent stem cells in drug development. Clin Pharmacol Ther 89:655-661.

Kobayashi T, Yamaguchi T, Hamanaka S, Kato-Itoh M, Yamazaki Y, Ibata M, Sato H, Lee YS, Usui J, Knisely AS, Hirabayashi M, Nakauchi H. 2010. Generation of rat pancreas in mouse by interspecific blastocyst injection of pluripotent stem cells. Cell 142:787-799.

Li P, Tong C, Mehrian-Shai R, Jia L, Wu N, Yan Y, Maxson RE, Schulze EN, Song H, Hsieh CL, Pera MF, Ying QL. 2008. Germline competent embryonic stem cells derived from rat blastocysts. Cell 135:1299-1310.

Lieb JD, Beck S, Bulyk ML, Farnham P, Hattori N, Henikoff S, Liu XS, Okumura K, Shiota K, Ushijima T, Greally JM. 2006. Applying whole-genome studies of epigenetic regulation to study human disease. Cytogenet Genome Res 114:1-15.

Lunney JK. 2007. Advances in swine biomedical model genomics. Int J Biol Sci 3:179-184.

Matsunari H, Onodera M, Tada N, Mochizuki H, Karasawa S, Haruyama E, Nakayama N, Saito H, Ueno S, Kurome M, Miyawaki A, Nagashima H. 2008. Transgenic-cloned pigs systemically expressing red fluorescent protein, Kusabira-Orange. Cloning Stem Cells 10:313-323.

Meissner A, Mikkelsen TS, Gu H, Wernig M, Hanna J, Sivachenko A, Zhang X, Bernstein BE, Nusbaum C, Jaffe DB, Gnirke A, Jaenisch R, Lander ES. 2008. Genome-scale DNA methylation maps of pluripotent and differentiated cells. Nature 454:766-770.

Montserrat N, Bahima EG, Batlle L, Häfner S, Rodrigues AM, González F, Izpisúa Belmonte JC. 2011. Generation of pig iPS cells: A model for cell therapy. J Cardiovasc Transl Res 4:121-130.

Nagashima H, Giannakis C, Ashman RJ, Nottle MB. 2004. Sex differentiation and germ cell production in chimeric pigs produced by inner cell mass injection into blastocysts. Biol Reprod 70:702-707.

Nagy A, Rossant J. 1993. Production of completely ES cell-derived fetuses. In: Joyner AL, editor. Gene targeting: a practical approch. UK: IRL Press. p 147-179.

Niwa H, Miyazaki J, Smith AG. 2000. Quantitative expression of Oct-3/4 defines differentiation, dedifferentiation or self-renewal of ES cells. Nat Genet 24:372-376.

Okita K, Ichisaka T, Yamanaka S. 2007. Generation of germline-competent induced pluripotent stem cells. Nature 448:313-317.

Okita K, Yamanaka S. 2011. Induced pluripotent stem cells: opportunities and challenges. Philos Trans R Soc Lond B Biol Sci 366:2198-2207.

Petters RM. 1994. Transgenic livestock as genetic models of human disease. Reprod Fertil Dev 6:643-645.

Prather RS, Hawley RJ, Carter DB, Lai L, Greenstein JL. 2003. Transgenic swine for biomedicine and agriculture. Theriogenology 59:115-123.

Rodríguez A, Allegrucci C, Alberio R. 2012. Modulation of pluripotency in the porcine embryo and iPS cells. PLoS One 7:e49079.

Sakaki-Yumoto M, Kobayashi C, Sato A, Fujimura S, Matsumoto Y, Takasato M, Kodama T, Aburatani H, Asashima M, Yoshida N, Nishinakamura R. 2006. The murine homolog of SALL4, a causative gene in Okihiro syndrome, is essential for embryonic stem cell proliferation, and cooperates with Sall1 in anorectal, heart, brain and kidney development. Development 133:3005-3013.

Sakamoto H, Suzuki M, Abe T, Hosoyama T, Himeno E, Tanaka S, Greally JM, Hattori N, Yagi S, Shiota K. 2007. Cell type-specific methylation profiles occurring disproportionately in CpG-less regions that delineate developmental similarity. Genes Cells 10:1123-1132.

Sato S, Yagi S, Arai Y, Hirabayashi K, Hattori N, Iwatani M, Okita K, Ohgane J, Tanaka S, Wakayama T, Yamanaka S, Shiota K. 2010. Genome-wide DNA methylation profile of tissue-dependent and differentially methylated regions (T-DMRs) residing in mouse pluripotent stem cells. Genes Cells 15:607-618.

Shiota K. 2004. DNA methylation profiles of CpG islands for cellular differentiation and development in mammals. Cytogenet Genome Res 105:325-334.

Shiota K, Kogo Y, Ohgane J, Imamura T, Urano A, Nishino K, Tanaka S, Hattori N. 2002. Epigenetic marks by DNA methylation specific to stem, germ and somatic cells in mice. Genes Cells 7:961-969.

Takahashi K, Tanabe K, Ohnuki M, Narita M, Ichisaka T, Tomoda K, Yamanaka S. 2007. Induction of pluripotent stem cells from adult human fibroblasts by defined factors. Cell 131:861-872.

Takahashi K, Yamanaka S. 2006. Induction of pluripotent stem cells from mouse embryonic and adult fibroblast cultures by defined factors. Cell 126:663-676.

Tesar PJ, Chenoweth JG, Brook FA, Davies TJ, Evans EP, Mack DL, Gardner RL, McKay RD. 2007. New cell lines from mouse epiblast share defining features with human embryonic stem cells. Nature 448:196-199.

Tsubooka N, Ichisaka T, Okita K, Takahashi K, Nakagawa M, Yamanaka S. 2009. Roles of Sall4 in the generation of pluripotent stem cells from blastocysts and fibroblasts. Genes Cells 14:683-694.

Usui J, Kobayashi T, Yamaguchi T, Knisely AS, Nishinakamura R, Nakauchi H. 2012. Generation of kidney from pluripotent stem cells via blastocyst complementation. Am J Pathol 180:2417-2426.

van der Spoel TI, Jansen of Lorkeers SJ, Agostoni P, van Belle E, Gyöngyösi M, Sluijter JP, Cramer MJ, Doevendans PA, Chamuleau SA. 2011. Human relevance of pre-clinical studies in stem cell therapy: systematic review and meta-analysis of large animal models of ischaemic heart disease. Cardiovasc Res 91:649-658.

West FD, Terlouw SL, Kwon DJ, Mumaw JL, Dhara SK, Hasneen K, Dobrinsky JR, Stice SL. 2010. Porcine induced pluripotent stem cells produce chimeric offspring. Stem Cells Dev 8:1211-1220.

West FD, Uhl EW, Liu Y, Stowe H, Lu Y, Yu P, Gallegos-Cardenas A, Pratt SL, Stice SL. 2011. Chimeric pigs produced from induced pluripotent stem cells demonstrate germline transmission and no evidence of tumor formation in young pigs. Stem Cells 10:1640-1643.

Wu Z, Chen J, Ren J, Bao L, Liao J, Cui C, Rao L, Li H, Gu Y, Dai H, Zhu H, Teng X, Cheng L, Xiao L. 2009. Generation of pig induced pluripotent stem cells with a drug-inducible system. J Mol Cell Biol 1:46-54.

Xu J, Pope SD, Jazirehi AR, Attema JL, Papathanasiou P, Watts JA, Zaret KS, Weissman IL, Smale ST. 2007.

Pioneer factor interactions and unmethylated CpG dinucleotides mark silent tissue-specific enhancers in embryonic stem cells. Proc Natl Acad Sci USA 104:12377-12382.

Yagi S, Hirabayashi K, Sato S, Li W, Takahashi Y, Hirakawa T, Wu G, Hattori N, Hattori N, Ohgane J, Tanaka S, Liu XS, Shiota K. 2008. DNA methylation profile of tissue-dependent and differentially methylated regions (T-DMRs) in mouse promoter regions demonstrating tissue-specific gene expression. Genome Res 18:1969-1978.

Xiong Z, Laird PW. 1997. COBRA: a sensitive and quantitative DNA methylation assay. Nucleic Acids Res 25: 2532-2534.

Zhao MT, Prather RS. 2011. The multi-potentiality of skin-derived stem cells in pigs. Theriogenology 75: 1372-1380.

Zhou L, Wang W, Liu Y, Fernandez de Castro J, Ezashi T, Telugu BP, Roberts RM, Kaplan HJ, Dean DC. 2011. Differentiation of induced pluripotent stem cells of swine into rod photoreceptors and their integration into the retina. Stem Cells 29:972-980.

Human Molecular Genetics, 2013, Vol. 22, No. 21
doi:10.1093/hmg/ddt287
Advance Access published on June 19, 2013

Dystrophin-deficient pigs provide new insights into the hierarchy of physiological derangements of dystrophic muscle

Nikolai Klymiuk[1,†], Andreas Blutke[3,†], Alexander Graf[2,†], Sabine Krause[4], Katinka Burkhardt[1], Annegret Wuensch[1], Stefan Krebs[2], Barbara Kessler[1], Valeri Zakhartchenko[1], Mayuko Kurome[1], Elisabeth Kemter[1], Hiroshi Nagashima[5], Benedikt Schoser[4], Nadja Herbach[3], Helmut Blum[2], Rüdiger Wanke[3], Annemieke Aartsma-Rus[6], Christian Thirion[4], Hanns Lochmüller[7,‡], Maggie C. Walter[4,‡] and Eckhard Wolf[1,2,‡,*]

[1]Chair for Molecular Animal Breeding and Biotechnology, [2]Laboratory for Functional Genome Analysis (LAFUGA), Gene Centre, [3]Institute of Veterinary Pathology, Centre for Clinical Veterinary Medicine and [4]Friedrich-Baur-Institute, Department of Neurology, LMU Munich, Germany, [5]Laboratory of Developmental Engineering, Meiji University, Kawasaki, Japan, [6]DMD Genetic Therapy Group, Department of Human Genetics, Leiden University Medical Centre, The Netherlands and [7]Institute of Genetic Medicine, Newcastle University, Newcastle upon Tyne, UK

Received March 21, 2013; Revised and Accepted June 14, 2013

Duchenne muscular dystrophy (DMD) is caused by mutations in the X-linked dystrophin (*DMD*) gene. The absence of dystrophin protein leads to progressive muscle weakness and wasting, disability and death. To establish a tailored large animal model of DMD, we deleted *DMD* exon 52 in male pig cells by gene targeting and generated offspring by nuclear transfer. DMD pigs exhibit absence of dystrophin in skeletal muscles, increased serum creatine kinase levels, progressive dystrophic changes of skeletal muscles, impaired mobility, muscle weakness and a maximum life span of 3 months due to respiratory impairment. Unlike human DMD patients, some DMD pigs die shortly after birth. To address the accelerated development of muscular dystrophy in DMD pigs when compared with human patients, we performed a genome-wide transcriptome study of biceps femoris muscle specimens from 2-day-old and 3-month-old DMD and age-matched wild-type pigs. The transcriptome changes in 3-month-old DMD pigs were in good concordance with gene expression profiles in human DMD, reflecting the processes of degeneration, regeneration, inflammation, fibrosis and impaired metabolic activity. In contrast, the transcriptome profile of 2-day-old DMD pigs showed similarities with transcriptome changes induced by acute exercise muscle injury. Our studies provide new insights into early changes associated with dystrophin deficiency in a clinically severe animal model of DMD.

INTRODUCTION

Duchenne muscular dystrophy (DMD) is a severe X-linked disease that affects 1 in 3500 males. DMD is caused by loss-of-function mutations in the *DMD* gene (~2.5 Mb, 79 exons) that lead to a shift in its reading frame, out-of-frame transcripts and loss of the essential muscle cytoskeletal protein dystrophin (1). The hotspots for mutations are in the regions of exons 3–7 and of exons 45–55 (2). DMD is characterized by progressive muscle weakness and wasting: patients present first symptoms before the age of 5 years, lose ambulation around the age of 12 years and die of respiratory or heart failure in the second to fourth decade of life (3).

*To whom correspondence should be addressed at: Chair for Molecular Animal Breeding and Biotechnology, Gene Centre, LMU Munich, Feodor-Lynen-Str. 25, D-81377 Munich, Germany. Tel: +49 89218076800; Fax: +49 89218076849; Email: ewolf@lmu.de
†Equally contributing authors.
‡Equally contributing last authors.

While curative treatments are currently not available, genetic and pharmacological approaches are under investigation, some having advanced to early phase clinical trials (4–7).

Existing mouse (8–10) and dog (11) models have been instrumental to understand the pathophysiology of DMD and to develop therapeutic strategies, but have limitations with respect to resemblance of the clinical phenotype and/or the type of mutation (reviewed in 12).

The pig is an established model organism for biomedical research closely resembling the human size, anatomy and physiology (reviewed in 13). Importantly, gene targeting allows the generation of tailored large animal models, as exemplified by the cystic fibrosis pig (14). Here, we report the generation and the clinical, pathological and biochemical characterization of pigs with a targeted deletion of *DMD* exon 52, a frequent mutation in human DMD (15). Transcriptome profiling of skeletal muscle from 2-day-old and 3-month-old DMD pigs provided new insights into the hierarchy of physiological derangements of dystrophic muscle.

RESULTS

Generation of *DMD* exon 52 deficient pigs

A bacterial artificial chromosome (BAC; CH242-9G11) carrying the relevant part of the porcine *DMD* gene was modified by recombineering (16) to replace the region corresponding to human *DMD* exon 52 by a neomycin resistance cassette (Fig. 1A), which is expected to result in a frame shift in the transcript (15). Modified BACs were transfected into primary kidney cells from a 3-month-old male piglet, and cell clones occurring after positive selection were screened by quantitative polymerase chain reaction (PCR) for replacement of *DMD* exon 52. Eight of 381 cell clones (2.1%) were successfully targeted, and 2 of them were used for nuclear transfer. For each cell clone, a pregnancy was established by transfer of cloned embryos into recipient gilts. Four piglets of the first litter were life born, euthanized within 48 h and tissue samples were processed for histological characterization. Genotyping confirmed the absence of *DMD* exon 52 (Fig. 1B). Two piglets of the second litter died during birth due to an obstetric complication, while the other two piglets (#1263, #1264; Fig. 1C) were delivered by caesarean section and survived. *DMD* exon 52 was deleted in these two piglets (Fig. 1B).

DMD exon 52 deficient pigs lack dystrophin and show reduced levels of dystrophin-associated proteins

The *DMD* transcript profile in skeletal muscle was analysed by RNA-sequencing (RNA-Seq). In the DMD samples, exon 52 sequences were entirely missing, but junctions from exons 51 to 53 were detected, leading to a +1 frame shift and two stop codons in exon 53 and four stop codons in exon 54 (Supplementary Material, Fig. S1).

Two monoclonal antibodies against different human dystrophin epitopes showed normal dystrophin staining of muscle fibres of a neonatal WT piglet, whereas in DMD piglets dystrophin staining was negative (Fig. 1D), reflecting the situation in the majority of human DMD patients (17) (Supplementary Material, Fig. S2). A monoclonal spectrin-specific antibody showed membrane integrity of muscle fibres in WT and DMD piglets (Fig. 1D). Immunoblot analysis confirmed the absence of dystrophin in skeletal muscle of DMD piglets (Fig. 1E).

Since dystrophin-associated proteins (DAPs) are reduced in DMD patients (reviewed in 18), we evaluated the abundance of α-sarcoglycan and β-dystroglycan in skeletal muscle of DMD piglets by immunofluorescence analysis. The levels of both DAPs were clearly reduced in DMD pigs as in DMD patients (Supplementary Material, Fig. S2).

Dystrophin-deficient pigs exhibit striking muscle weakness

DMD piglets #1263 and #1264 showed reduced mobility when compared with age-matched WT controls, but were able to move and feed on their own. At the age of 3 days, their serum creatine kinase (CK) levels were largely elevated (1649 and 2117 versus 210 ± 112 U/l in 5 age-matched WT controls). #1264 died from an intestinal infection at the age of 2 weeks.

Locomotion studies of DMD pig #1263 were performed at the age of 9 weeks using a size-matched WT pig as a control. The mobility of the DMD pig was disturbed in all three gaits (walk, trot, gallop), with shortened strides and stiff movements being the most prominent features (Supplementary Material, Video S1). While the WT pig easily mastered repeatedly jumping up and down a platform (height 25 cm), the DMD pig failed to climb the platform (Fig. 1F and Supplementary Material, Video S1), demonstrating striking muscle weakness.

Severity of the DMD phenotype correlates with birth weight

To address the clinical phenotype of DMD pigs systematically, we performed a second series of nuclear transfer experiments, resulting in a total of 22 DMD piglets ($n = 9$, 9 and 4 per litter). The cloned piglets showed a large variation in birth weight, which is a finding known to be associated with nuclear transfer technology (19) and is not related to the *DMD* mutation. Interestingly, we observed a negative correlation between birth weight and life expectancy (Fig. 2A). Animals with a birth weight of more than 1200 g died within the first few days. DMD piglets with the highest birth weight (1820–1980 g) were most severely affected and could not move at all (Fig. 2A and Supplementary Material, Video S2). The clinical symptoms suggested muscle weakness and breathing problems as primary causes of death. In contrast, the life expectancy of five animals with a relatively low birth weight was in the range of 3 months, as observed for DMD piglet #1263 from the first SCNT series. At the age of 4 weeks, their serum CK values ranged between 21 000 and 63 000 U/l. Additional locomotion studies performed in two 10-week-old DMD pigs confirmed the difficulties in running and climbing (Supplementary Material, Video S3).

DMD pigs exhibit fulminant progressive muscular dystrophy

DMD pigs of different ages and age-matched WT pigs were subjected to systematic pathological analysis. Grossly, DMD pigs displayed pale skeletal muscles of moist texture, with multifocal areas of pale discolouration, especially in the diaphragm and intercostal musculature. Histological examination revealed a